

# PCCP

Physical Chemistry Chemical Physics

www.rsc.org/pccp

Volume 12 | Number 2 | 14 January 2010 | Pages 293–536

Published on 07 November 2009. Downloaded by Pennsylvania State University on 10/05/2016 22:45:14.



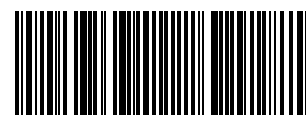
ISSN 1463-9076

**COVER ARTICLE**

Sokolov *et al.*  
Towards understanding of shape formation mechanism of mesoporous silica particles

**PERSPECTIVE**

Foster and Sohlberg  
Empirically corrected DFT and semi-empirical methods for non-bonding interactions



1463-9076(2010)12:2;1-W

# Towards understanding of shape formation mechanism of mesoporous silica particles†

Dmytro O. Volkov,<sup>a</sup> James Benson,<sup>a</sup> Yaroslav Y. Kievsky<sup>a</sup> and Igor Sokolov<sup>\*abc</sup>

Received 23rd August 2009, Accepted 1st October 2009

First published as an Advance Article on the web 7th November 2009

DOI: 10.1039/b917424a

Growth of even simple crystals is a rather hard problem to describe because of the non-equilibrium nature of the process. Meso(nano)porous silica particles, which are self-assembled in a sol-gel template synthesis, demonstrate an example of shapes of high complexity, similar to those observed in the biological world. Despite such complexity, here we present the evidence that at least a part of the formation of these shapes is an equilibrium process. We demonstrate it for an example of mesoporous fibers, one of the abundant shapes. We present a quantitative proof that the fiber free energy is described by the Boltzmann distribution, which is predicted by the equilibrium thermodynamics. This finding may open up new ground for a quantitative description of the morphogenesis of complex self-assembled shapes, including biological hierarchy.

## 1. Introduction

Emerging of various complex shapes in nature has attracted the attention of scientists for centuries. The morphogenesis of liquid crystals, a famous example of self-organization in a non-biological milieu, has been studied since 1888.<sup>1,2</sup> A century ago, Haeckel<sup>3,4</sup> called it “Studies of Inorganic Life” because of its striking resemblance to complex biological morphologies. The prediction of particle shapes, including the shapes observed in the biological world,<sup>5–7</sup> is one of the fundamental yet unsolved problems. Despite being long-standing and important, the problem of shape formation has not been solved, even for the growth of simple crystals. The major difficulty in understanding the growth is that a typical shape formation mechanism is not an equilibrium process, and kinetics is usually the dominant mechanism in the shaping control. As a result, successful prediction of the shape has been done so far through computer molecular simulations for relatively simple monomolecular crystals.<sup>8</sup>

Mesoporous (sometimes called nanoporous) silica particles,<sup>9–11</sup> which are self-assembled in a sol-gel template synthesis, demonstrate an example of shapes of high complexity, similar those observed in biological world. These shapes can extend up to a few hundred microns and form mesoporous thin films,<sup>8,12–17</sup> spheres,<sup>18–20</sup> curved shaped solids,<sup>9,13</sup> tubes,<sup>21,22</sup> rods and fibers,<sup>9,13,23</sup> membranes,<sup>24</sup> and monoliths.<sup>25</sup> Fig. 1 shows an example of the variability of shape complexities.

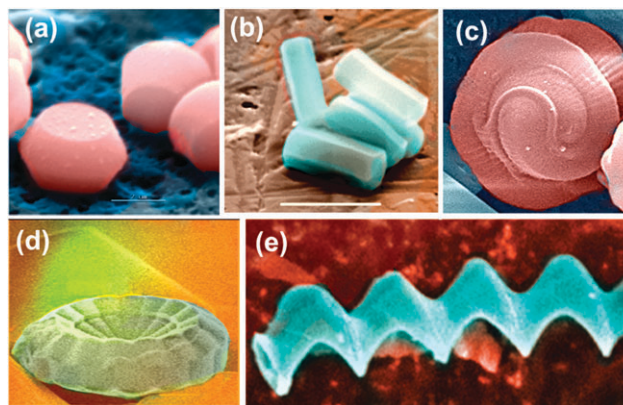


**Fig. 1** Examples of mesoporous silica shapes. SEM images of (a) discoids, (b) fibers,<sup>26</sup> (c,d) “seashells”,<sup>27</sup> and (e) helix.<sup>28</sup> The particle sizes vary from single to hundreds of microns. All shapes have hexagonal nanochannels of  $\sim 3$  nm in diameter. Highlighting with colours is artificial.

## 2. Experimental

### 2.1 Materials

Cetyltrimethylammonium chloride (CTACl, 25 wt% aqueous solution) and tetraethylorthosilicate (TEOS, 99.999%) precursors were obtained from Aldrich. Hydrochloric acid (HCl, 37.6 wt% aqueous solution, J T Baker) Solutions were diluted with either distilled or deionized water (18 M $\Omega$ -cm, MilliQ Ultrapure). All chemicals were used as received.

### 2.2 Synthesis

The acidic synthesis of the fibers at room temperature was described previously in ref. 26. Here we used the same idea of the synthesis although varying the temperature during the synthesis. The surfactant, acid, and ultrapure water

<sup>a</sup> Department of Physics, 8 Clarkson Ave., Clarkson University, Potsdam, NY 13699, USA. E-mail: isokolov@clarkson.edu

<sup>b</sup> Department of Chemical & Biomolecular Science, Clarkson University, Potsdam, NY 13699, USA

<sup>c</sup> Nanoengineering and Biotechnology Laboratories Center (NABLAB), Clarkson University, Potsdam, NY 13699, USA

† Electronic supplementary information (ESI) available: zoo of shapes indicating similarity in the formation mechanism, derivations and codes used in the paper. See DOI: 10.1039/b917424a



(18 M $\Omega$ -cm, MilliQ Ultrapure) were mixed in a plastic bottle (HDPE), stirred first at room temperature (20 °C) for 1 min, and then placed in either a refrigerator (4 °C) or into a water bath (20 °C and 35 °C) for 15 min. Thermally equilibrated TEOS (either at 4 °C, or 20 °C, or 35 °C) was added to the acidic solution of surfactant of corresponding temperature, and stirred for 30 s. The final molar composition of the reactants H<sub>2</sub>O:HCl:CTACl:TEOS was 100:9:0.22:0.13, respectively. The resulting solution was kept under quiescent conditions for 3 h at 4 °C, or 1 h at 20 °C, or 30 min at 35 °C, respectively. The material was collected by centrifugation (5 min, 3000 r/min, IEC Clinical Centrifuge), then resuspended in distilled water, and centrifuged again. The centrifugation and resuspension procedures were repeated.

### 2.3 Characterization

Characterization was done by electron microscopy (SEMs: JEOL JSM-6300, FEI Phenom; TEM: JEOL 2010). Using SEM images, we measure the radii of curvature, thicknesses and lengths of the fibers with Image Tool software (by University of Texas in San Antonio).

## 3. Results and discussion

Relatively recently, it has been proposed<sup>26,28,29</sup> that some details of the shapes observed for mesoporous silica could be explained as the defects typical for liquid crystals, the templates which were formed during the initial stages of the synthesis. Here we hypothesized that the shapes of particles themselves are formed in an equilibrium process driven by the minimization of energy and balancing it with entropy, *i.e.*, described by the Boltzmann distribution of its free energy. Here we demonstrate it for curved mesoporous fibers, Fig. 1b and Fig. 2.

The choice of fibers is justified by three reasons: (1) A variety of other mesoporous shapes can be obtained by just changing acidity of the fiber synthesis.<sup>30</sup> This indicates the universality of the formation mechanisms of the mesoporous shapes, including fibers. (2) The fibers are one of the abundant and fairly monodispersed shapes in the family. (3) These particles have the easiest geometry to process, which is needed to calculate their free energy. In principle, we could repeat the same study for any of the other shapes. However, it would require a substantially higher amount of work to process that data, and will supposedly be done in the future. From a practical point of view, the study of fibers is also interesting for the investigation of controlled release,<sup>31</sup> biological channels,<sup>32,33</sup> properties of interfacial water,<sup>34–36</sup> and the capillarity of rocks in geophysics,<sup>37–40</sup> *etc.*

To test our hypothesis about the thermodynamical equilibrium of the fiber free energy, we synthesized fibers at three different temperatures: 4, 20, and 35 °C. Fig. 2 shows certain differences in geometrical parameters of the fibers synthesized at those temperatures.

Higher magnification images reveal a hexagonal cross-section of all fibers, Fig. 3. Transmission electron microscopy (TEM, JEOL 2010) imaging of the fiber edges, also shown in Fig. 3, shows that the mesochannels are running along the fiber. X-Ray and gas adsorption (data not shown) confirm that

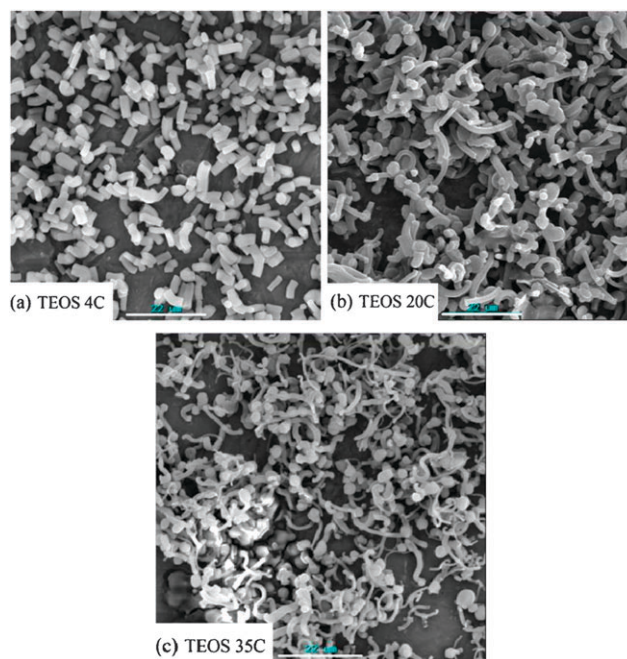


**Fig. 2** Scanning electron microscopy (SEM, FEI Phenom) images of mesoporous silica fibers synthesized at different temperatures: (a) 4 °C, (b) 20 °C, and (c) 35 °C. The synthesis of the fibers the temperature of 4 °C was described previously in ref. 27. The same synthesis was used here for the other temperatures. The only difference was in the synthesis time: for 3 h at 4 °C, 1 h at 20 °C, and 30 min at 35 °C.

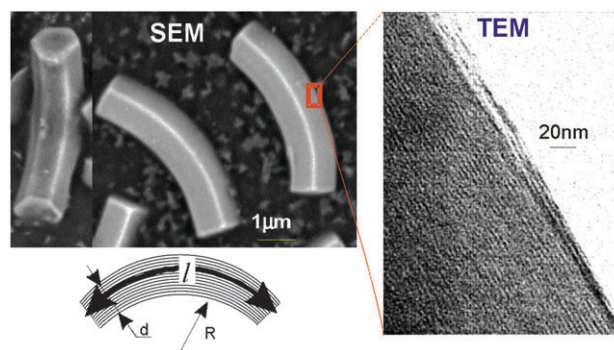


**Fig. 3** Representative SEM images show a hexagonal cross-section of fibers. Transmission electron microscopy (TEM) imaging of the fiber edge demonstrates that the nanochannels are running along the fiber. A schematic of a fiber shows the notations used in the text.

we are dealing with a hexagonal orientation (*p6mm*) of highly uniform nanoscopic channels of  $\sim 3$  nm.

Let us now show that the free energy of these fibers is described by the equilibrium thermodynamics, *i.e.*, Boltzmann distribution. Thermodynamics requires the chemical potential  $\mu$  to be constant for all shapes:

$$\mu = \mu^0 + k_B T \ln(X) = \text{const}, \quad (1)$$

where  $\mu^0$  is the free energy of a shape,  $X$  is the relative number/concentration of the shapes having free energy  $\mu^0$ ,  $T$  is the temperature and  $k_B$  is the Boltzmann constant.

Because the fibers inherit the internal pore structure of nematic liquid crystal template, their free energy may be

described by the Frank–Landau free energy formula<sup>41</sup> for nematic liquid crystals:

$$\mu^0 = \int_{\text{Volume}} \left( \frac{K_1}{2} (\text{div} \vec{n})^2 + \frac{K_2}{2} (\vec{n} \cdot \text{rot} \vec{n})^2 + \frac{K_3}{2} [\vec{n} \times \text{rot} \vec{n}]^2 \right) dv \quad (2)$$

where  $\vec{n}$  is a unit vector tangential to the nanochannels (similar to the director-field of the nematic crystal), and  $K_{1,2,3}$  are the elastic modulus values corresponding to splay, twist, and bend deformations, respectively. Because we do not observe a noticeable amount of fibers that are twisted around the axis of symmetry or splayed fibers, the terms with  $K_1$  and  $K_2$  vanish. It should be noted that surface energy appears not to play a noticeable role here because of the well defined hexagonal cross-section of the fibers (the role of surface tension is in particular in rounding the edges of the shapes – see ref. 42).

Integrating over the fiber gives the following result (see the ESI† for more detail):

$$\mu^0 = \frac{lK_3\sqrt{3}}{2R} \left[ d \ln \left[ \frac{d-4R}{3d-4R} \right] + 4R \ln \left[ \frac{4R}{4R-d} \right] - 2(d-2R) \ln \left[ \frac{d-4R}{2d-4R} \right] \right] \quad (3)$$

Here  $l$  is the length of a fiber,  $d$  is the diameter of the fiber,  $R$  is the radius of the bent fiber (Fig. 3).

Eqn (3) is derived for a particular orientation of the fiber shown in Fig. 3. However,  $\mu^0$  is virtually independent of the fiber orientation. It changes within 0.002% for the typical geometry of the fibers (see the ESI†). Therefore we do not specify the difference in the rotation angle when collecting geometries of the fibers in our measurements.

Rewriting eqn (1), one obtains the Boltzmann distribution law that we test

$$X(\mu^0, T) = A(T) \exp[-\mu^0/k_B T], \quad A(T) = \exp[\mu/k_B T]. \quad (4)$$

Taking the SEM images (but with a lesser number of particles for the ease of processing), one can find the required geometrical parameters,  $l$ ,  $R$ ,  $d$  to calculate the free energy  $\mu^0$ .

The processed data are presented in Fig. 4 as histograms. It shows the logarithm of the number of particles with particular  $\mu^0/K_3$ . The Boltzmann distribution given by eqn (4) should be represented by a straight line. To compare with the Boltzmann distribution, it is drawn using  $K_3$  taken as the most probable for the observed  $\mu^0$  from the point of view of the Boltzmann distribution (it is found by the maximum likelihood method). One can see a very good agreement of the observed statistics with the Boltzmann distribution. Some small deviation is observed for large free energies, *i.e.*, for the fibers of high curvature. This is presumably explained by the fact that the ends of such fibers can be pulling towards each other by van der Waals force, which is not taken into account in the Frank–Landau formula (2). This additional force will contribute to the increase of fiber curvature, and consequently, to higher internal energy. Ultimately, this force and the Brownian motion bring the fiber ends together, so the fibers are “glued” together (Fig. 5).

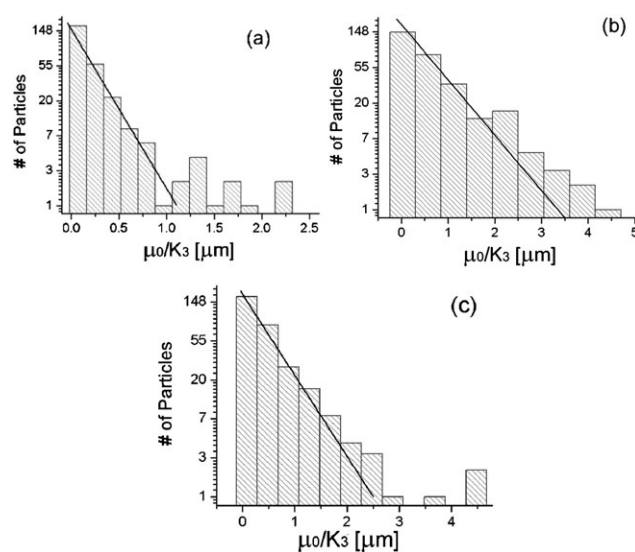


**Fig. 4** Distributions of free energy for mesoporous silica fibers synthesized at different temperatures: (a) 4 °C, (b) 20 °C, and (c) 35 °C. The straight lines correspond to the Boltzmann distribution with parameter  $K_3$  calculated as the most probable for the assumed Boltzmann distribution.

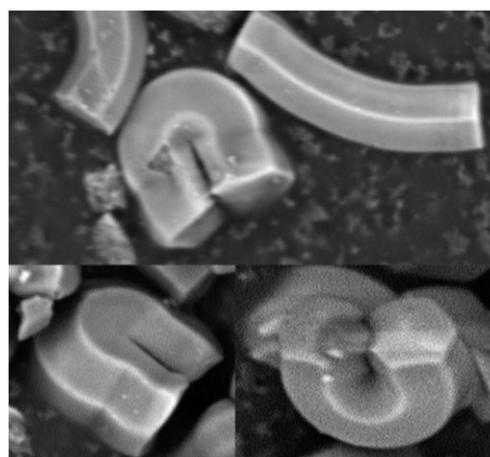


**Fig. 5** Typical SEM images of high curvature fibers with the ends “glued” together.

The reason for the shaping mechanism to be an equilibrium process is presumably as follows. Freshly formed mesoporous silica particles, including fibers, are sufficiently soft. Consequently, they can be entropically bent by Brownian motion. Condensation of silica goes through the increase of the number of cross-linking  $-\text{Si}-\text{O}-\text{Si}-$  vs.  $-\text{Si}-\text{OH}$   $\text{OH}-\text{Si}-$  bonds.<sup>43</sup> It results in the increase of fiber rigidity. However, this process is relatively slow (from tens of minutes to days), and the shape free energies have sufficient time to be equilibrated with the thermal bath of the environment. Consequently, the free energy of the fibers is described by the Boltzmann distribution. In other words, equilibrium thermodynamics can be considered as an adiabatic approximation for the formation of the fiber shapes. As time goes on, condensing silica becomes more rigid, and at one point, the Brownian motion cannot “bend” the fibers anymore. The fibers “quench” their shapes at that point.

## 4. Conclusion

Here we presented the evidence that at least a part of formation of mesoporous silica shapes is an equilibrium process. We present a quantitative proof that the fiber free energy is described by the Boltzmann distribution, which is predicted by the equilibrium thermodynamics. This was demonstrated for the syntheses of fibers at three different temperatures.

It is worth noting that the same reason is applicable to the synthesis of all mesoporous particles of other shapes. Moreover, a similar slow rigidification takes place for the growth of seashells, diatoms, bones, *etc.* Therefore, we believe that this finding may open up new ground for the quantitative description of the morphogenesis of complex self-assembled shapes, including biological hierarchy.

I. S. acknowledges support from NSF (grant CBET 0755704) and ARO (grant W911NF-05-1-0339).

## References

- 1 F. Reinitzer, *Monatsh. Chem.*, 1888, **9**, 421.
- 2 O. Lehmann, *Die Flüssige Kristalle*, Akademische Verlags-gesellschaft M.B.H., Leipzig, 1911.
- 3 E. Haecckel, *Generelle Morphologie*, 1866, vol. 2, Georg Reimer, Berlin.
- 4 A. L. Makay, *Forma*, 1999, **14**, 11–29.
- 5 N. Bessonov, N. Morozova and V. Volpert, *Bull. Math. Biol.*, 2008, **70**, 868–893.
- 6 K. J. Niklas, *J. Morphol.*, 1994, **219**, 243–246.
- 7 D. Savic, *J. Theor. Biol.*, 1995, **172**, 299–303.
- 8 S. Piana, M. Reyhani and J. D. Gale, *Nature*, 2005, **438**, 70–73.
- 9 G. A. Ozin, H. Yang, I. Yu. Sokolov and N. Coombs, *Adv. Mater.*, 1997, **9**, 662–667.
- 10 S. Oliver, A. Kuperman, N. Coombs, A. Lough and G. A. Ozin, *Nature*, 1995, **378**, 47–50.
- 11 H. Yang, N. Coombs and G. A. Ozin, *Nature*, 1997, **386**, 692.
- 12 I. Sokolov, H. Yang, G. A. Ozin and G. S. Henderson, *Adv. Mater.*, 1997, **9**, 917–921.
- 13 H. Yang, G. A. Ozin and C. T. Kresge, *Adv. Mater.*, 1998, **10**, 883–887.
- 14 H. Yang, I. Yu. Sokolov, N. Coombs, O. Dag and G. A. Ozin, *J. Mater. Chem.*, 1997, **7**, 1755–1761.
- 15 H. Yang, N. Coombs, I. Yu. Sokolov and G. A. Ozin, *J. Mater. Chem.*, 1997, **7**, 1285–1290.
- 16 H. Yang, N. Coombs, I. Yu. Sokolov and G. A. Ozin, *Nature*, 1996, **381**, 589–592.
- 17 D. Zhao, P. Yang, N. Melosh, J. Feng, B. F. Chmelka and G. D. Sucky, *Adv. Mater.*, 1998, **10**, 1380–1385.
- 18 H. Yang, G. Vovk, N. Coombs, I. Sokolov and G. A. Ozin, *J. Mater. Chem.*, 1998, **8**, 743–750.
- 19 S. Schacht, Q. Huo, I. G. Voigt-Martin, G. D. Stucky and F. Schuth, *Science*, 1996, **273**, 768–771.
- 20 M. Grun, I. Lauer and K. K. Unger, *Adv. Mater.*, 1997, **9**, 254–257.
- 21 M. Yang, I. Yu. Sokolov, N. Coombs, C. T. Kresge and G. A. Ozin, *Adv. Mater.*, 1999, **11**, 1427–1431.
- 22 F. Kleitz, F. Marlow, G. D. Stucky and F. Schuth, *Chem. Mater.*, 2001, **13**, 3587–3595.
- 23 P. Schmidt-Winkel, P. Yang, D. I. Margolese, B. F. Chmelka and G. D. Stucky, *Adv. Mater.*, 1999, **11**, 303–307.
- 24 D. Zhao, P. Yang, B. F. Chmelka and G. D. Stucky, *Chem. Mater.*, 1999, **11**, 1174–1178.
- 25 N. A. Melosh, P. Davidson and B. F. Chmelka, *J. Am. Chem. Soc.*, 2000, **122**, 823–829.
- 26 S. M. Yang, H. Yang, N. Coombs, I. Yu. Sokolov, C. T. Kresge and G. A. Ozin, *Adv. Mater.*, 1999, **11**, 52–55.
- 27 Y. Kievsky and I. Sokolov, *IEEE Trans. Nanotechnol.*, 2005, **4**, 490–494.
- 28 S. P. Naik and I. Sokolov, *Solid State Commun.*, 2007, **144**, 437–440.
- 29 I. Yu. Sokolov, H. Yang, G. A. Ozin and C. T. Kresge, *Adv. Mater.*, 1999, **11**, 636.
- 30 I. Sokolov and Y. Kievsky, *Stud. Surf. Sci. Catal.*, 2005, **156**, 433–443.
- 31 Y. Y. Kievsky, B. Carey, S. Naik, N. Mangan, D. ben-Avraham and I. Sokolov, *J. Chem. Phys.*, 2008, **128**, 151102.
- 32 M. S. P. Sansom, I. D. Kerr, J. Breed and R. Sankararamakrishnan, *Biophys. J.*, 1996, **70**, 693–702.
- 33 R. M. Lynden-Bell and J. C. Rasaiah, *J. Chem. Phys.*, 1996, **105**, 9266–9280.
- 34 P. Gallo, M. Rovere, M. A. Ricci, C. Hartnig and E. Spohr, *Europhys. Lett.*, 2000, **49**, 183–188.
- 35 P. Gallo, M. Rovere and E. Spohr, *Phys. Rev. Lett.*, 2000, **85**, 4317–4320.
- 36 A. Poynor, L. Hong, I. K. Robinson, S. Granick, Z. Zhang and P. A. Fenter, *Phys. Rev. Lett.*, 2006, **97**, 266101.
- 37 C. L. Perrin, P. M. Tardy, K. S. Sorbie and J. C. Crawshaw, *J. Colloid Interface Sci.*, 2006, **295**, 542–550.
- 38 R. D. Hazlett, *Transport Porous Media*, 1995, **20**, 1573–1634.
- 39 A. P. Radlinski, M. A. Ioannidis, A. L. Hinde, M. Hainbuchner, M. Baron, H. Rauch and S. R. Kline, *J. Colloid Interface Sci.*, 2004, **274**, 607–612.
- 40 Y. Q. Song, S. Ryu and P. N. Sen, *Nature*, 2000, **406**, 178–181.
- 41 L. D. Landau, L. P. Pitaevskii, A. M. Kosevich and E. M. Lifshitz, *Theory of Elasticity*, Butterworth-Heinemann, Oxford, 3rd edn, 1986.
- 42 G. Cao, *Nanostructures and Nanomaterials: Synthesis, Properties & Applications*, Imperial College Press, London, 2004.
- 43 R. K. Iler, *The Chemistry of Silica: Solubility, Polymerization, Colloid and Surface Properties and Biochemistry of Silica*, Wiley, John & Sons Incorporated, New York, 1979.